Spin dynamics in MgO based magnetic tunnel junctions with dynamical exchange coupling

Zhengren Yan,[1] Xingtao Jia,[2,*] Pingping Wu,[2] and Minghui Qin[1,†]

[1] *Institute for Advanced Materials, South China Academy of Advanced Optoelectronics and Guangdong Provincial Key Laboratory of Quantum Engineering and Quantum Materials, South China Normal University, Guangzhou 510006, China*

[2] *School of Physics and Electronic Information Engineering, Henan Polytechnic University, Jiaozuo 454000, China*

(Dated: May 2, 2019)

We study the spin dynamics in Fe|MgO|Fe tunnel junction with the dynamical exchange coupling by coupled Landau-Lifshitz-Gilbert equations. The effects of spin pumping on the spin dynamics are investigated in detail. It is observed that the spin pumping can stabilize a quasi-antiparallel state rather than a quasi-parallel one. More interestingly, our work suggests that the spin pumping torque can efficiently modulate the magnetization, similar to the thermal-bias-driven and electric-bias-driven spin torques.

PACS numbers: 72.25.Ba, 75.78.Jp, 85.75.Dd, 85.75.-d

I. INTRODUCTION

The study of dynamic behaviors in magnetic structures is essential for the spintronic applications.[1–6] The enhanced magnetic dampings $\sim 10^{-1}$ induced by spin pumping have been reported in $Ni_{80}Fe_{20}$ (Py) films in contact with the nonmagnetic metals Cu, Pd, Ta, and Pt, respectively.[7–9] The giant magnetic damping is of one order larger than that in the bulk system, and has a significant effect on the dynamic behaviors. Besides, due to the reported giant magnetoresistance (MR)[10–12] and tunnel magneto-Seebeck ratio (TMS),[13–20] MgO-based magnetic tunnel junctions (MTJs) are attracting much attentions in logic unit and memory applications.[18] During the past a few years, spin dynamics in ultrathin Fe|MgO|Fe MTJs with thermal spin transfer torque (TSTT) have been systemically studied by phenomenological Landau-Lifshitz-Gilbert (LLG) calculations.[21,22] Most recently, spin pumping has been reported experimentally in magnetic trilayer structures with an MgO barrier.[24] Furthermore, the enhanced magnetic damping in this system could be rather strong and very important in spin dynamics.[23] As a matter of fact, an obvious effect of spin pumping through AlO barrier has been observed in earlier work, partially suggesting that the effect of spin pumping through MgO could not be simply ignored.[25,26] Importantly, a giant enhancement of spin pumping from the two ferromagnetic layers embedded in a normal metal was predicted recently.[27,28] Thus, the effect of the enhanced magnetic damping resulted from spin scattering at interface deserves to be investigated in detail.

Normally, spin current is preferentially used to drive the dynamics of magnetic structure,[29–31] which can be induced by electronic voltage and temperature. The electronic voltage induced spin transfer torque (STT) has been well studied in earlier works,[32–36] and the thermal induced STT[37–45] attracted much attentions most recently. It is demonstrated that a temperature field has an effect on generating the torque similar to that of a magnetic field. Specifically, strong TSTT induced by a large temperature gradient across ultrathin MgO tunnel barriers can considerably change the switching field of the MTJ.[44] Furthermore, various methods of enhancing TSTT have been proposed.[46–50] For example, external driving forces such as electronic voltage have been proven to tune the thermal effect on ferromagent-insulator (F|I) interface by the band scissoring engineering.[18,51]

In addition, a processing magnetization in ferromagnet can pump spin current and drives the spin dynamics,[52] and its amplitude is dependent on energy gain from static magnetic field or microwave radio frequency field. When the ferromagnet is contacting with a normal metal, an enhanced spin pumping is expected.[53] In fact, in a ferromagnet|normal metal|ferromagnet (FM|NM|FM) structure, the spin current pumped from the processing magnetization can be used to modulate the free magnetization when the dynamical exchange coupling[54–57] is strong enough. For example, the synchronizing procession[54–57] induced by the dynamic exchange coupling in the magnetic bilayers has been observed in earlier experiments, demonstrating the important role of the spin pumping on the spin dynamics. However, there is still an open question that how the spin pumping affects on the spin dynamics in MgO-based magnetic tunnel junctions, which is important to understand the physics and may provide new insights on the corresponding device design. Hence, detailed theoretical works on this subject are urgently needed.

In this work, we focus on the spin dynamics in Fe|MgO|Fe tunnel junction considering the dynamical exchange coupling by a set of coupled LLG equations. Free spin dynamics studies show that the quasi-antiparallel (AP) structure is more stable than the quasi-parallel (P) structure in the presence of spin pumping. Furthermore, the effects of various parameters such as processing cone angle, asymmetric effective field, and external spin torque on the magnetic state switching are investigated in detail.

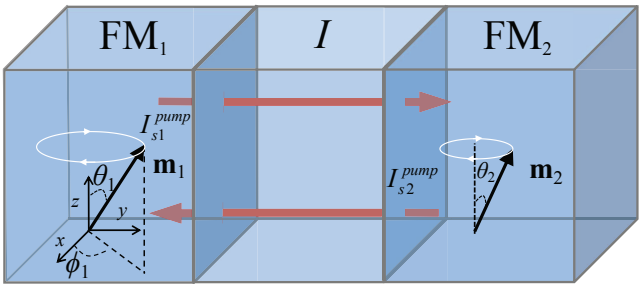

FIG. 1. Schematic $FM_1|I|FM_2$ MTJ used in the calculations. When both the magnetizations precess, spin currents $I_{s,1}^{pump}$ pumped from $\mathbf{m}_1$ and $I_{s,2}^{pump}$ from $\mathbf{m}_2$ pass across the insulator (I) and are absorbed by $\mathbf{m}_2$ and $\mathbf{m}_1$, respectively.

The manuscript is organized as follows. In Sec. II, we give the spin dynamic model with the dynamical exchange coupling. In Sec. III, the numerical results including free spin dynamics, spin dynamics under a magnetic field, and spin dynamics with the external spin torque are given and discussed in detail. Sec. IV is the summary.

II. SPIN DYNAMIC MODEL

Considering a magnetic structure with the dynamical exchange coupling, as shown in Fig. 1, the dynamics of the magnetization of both layers can be described by the LLG equation[54–57]

$$\frac{d\mathbf{m}_i}{d\tau} + \alpha_0 \mathbf{m}_i \times \frac{d\mathbf{m}_i}{d\tau} = \vec{\Gamma}_i^a + \vec{\Gamma}_i^P + \vec{\Gamma}_i^T, \qquad (1)$$

where $\vec{\Gamma}_i^a$, $\vec{\Gamma}_i^P$, and $\vec{\Gamma}_i^T$ are the torques exerted on magnetic vector $\mathbf{m}_i$ and α_0 is the intrinsic magnetic damping coefficient resulted from the spin-orbital coupling. $\vec{\Gamma}^a$ originates from the effective filed and planar anisotropy,[58] and $\vec{\Gamma}_i^P = \alpha_i'[\mathbf{m}_j \times (d\mathbf{m}_j/d\tau) - \mathbf{m}_i \times (d\mathbf{m}_i/d\tau)]$ with $i = 1(2)$ and $j = 2(1)$ is the net pumping torque related to the enhanced magnetic damping coefficient α_i' from the interfacial scattering, which can be estimated from the scattering theory.[7] In this work, α_i' is set to be constant for simplicity, although the enhancement of the spin damping generally depends on the relative angle of the magnetizations.[59] $\vec{\Gamma}_i^T = \tau_\parallel \mathbf{m}_1 \times (\mathbf{m}_2 \times \mathbf{m}_1) + \tau_\perp \mathbf{m}_1 \times \mathbf{m}_2$ is the torque responded to the electronic voltage or thermal bias. Expressing the above equations in spherical coordinates, we obtain two differential equations for the polar angle θ and azimuthal angel ϕ:

$$\begin{aligned} \dot{\theta}_i &= \dot{\theta}_i^a + \dot{\theta}_i^P + \dot{\theta}_i^T \\ \dot{\phi}_i &= \dot{\phi}_i^a + \dot{\phi}_i^P + \dot{\phi}_i^T \end{aligned} \qquad (2)$$

with

$$\begin{aligned} \dot{\theta^a} &= -\alpha k \sin\theta\cos\theta - h_p \sin\theta\cos\phi(\sin\phi + \alpha\cos\theta\cos\phi) \\ \dot{\theta^P} &= -[A/\sin\theta + \alpha(B\sin\phi - C\cos\phi)] \\ \dot{\theta^T} &= -[h_T^z/\sin\theta + \alpha(h_T^x\sin\phi - h_T^y\cos\phi)] \\ \dot{\phi^a} &= -k\cos\theta - h_p\cos\phi(\cos\phi\cos\theta - \alpha\sin\phi) \\ \dot{\phi^P} &= [\alpha A/\sin^2\theta - (B\sin\phi - C\cos\phi)/\sin\theta] \\ \dot{\phi^T} &= [\alpha h_T^z/\sin^2\theta - (h_T^x\sin\phi - h_T^y\cos\phi)/\sin\theta] \end{aligned}$$

where $\dot{()} = d()/d\tau$ with a dimensionless time $\tau = t\Omega_K/(1+\alpha_0^2)$ estimated from the the ferromagnetic resonance frequency $\Omega_K = \gamma H_K$ with the effective field H_K, $A_i = \alpha_i'\dot{\phi}_j sin^2\theta_j$, $B_i = -\alpha_i'(\dot{\theta}_j sin\phi_j + \dot{\phi}_j cos\phi_j sin\theta_j cos\theta_j)$, $C_i = \alpha_i'(\dot{\theta}_j cos\phi_j - \dot{\phi}_j sin\phi_j sin\theta_j cos\theta_j)$, $h_P = K_P/K$ is the dimensionless planar anisotropy field with the planar anisotropy constant K_P normalized by the uniaxial anisotropy constant $K = M_s H_K/2$, $h_T = \Gamma^T/2Kd$ is the dimensionless spin torque related to the thickness of free magnetization d, $k_i = H_{K,i}/H_{K,1}$ is the normalized effective filed, and $\alpha = \alpha_0 + \alpha'$ is the total magnetic damping coefficient. The angle-dependent spin torques responded to the driving force are parameterized by $\tau_{\parallel(\perp)}/\tau_{\parallel(\perp)}^{(0)} = [\Lambda_{\parallel(\perp)}\cos^2(\theta'/2) + (1/\Lambda_{\parallel(\perp)})\sin^2(\theta'/2)]^{-1}$, where θ' is the relative angle between $\mathbf{m}_1$ and $\mathbf{m}_2$, $\tau^{(0)}$ is the spin torque at the relative angle of 90 degree, and Λ[60] is slonczewski's asymmetric parameter.

III. NUMERICAL RESULTS AND DISCUSSION

For a free symmetric magnetic structure (without any applied spin torque) such as the MTJ depicted in Fig. 1, the spin-current pumped by one processing magnetization would drive a coherent procession of the other magnetization.[54–57] However, when the enhanced magnetic damping coefficient is negligible, the spin current would be absorbed by itself and could not inject into the insulator, leading to the fact that the dynamics of the two magnetizations across the insulator are independent on each other. There are two factors contribute to the coherent procession of the magnetizations. One is the enhanced magnetic damping coefficient which determines the amplitude of the spin current and the critical time at which the two magnetizations begin to process with a same tune. The other is the intrinsic magnetic damping coefficient which stabilizes the magnetizations to the focuses.

In this part, we study another important model of the asymmetric sandwiched magnetic structure with dynamical exchange coupling. The asymmetry can be introduced by designing structures with different magnets, different thickness, different chemical environments, and/or even exerting a local magnetic field on one FM layer only.

First, we set the magnetic parameters from the CoFe|MgO|CoFe MTJs for both magnetizations. Specif-

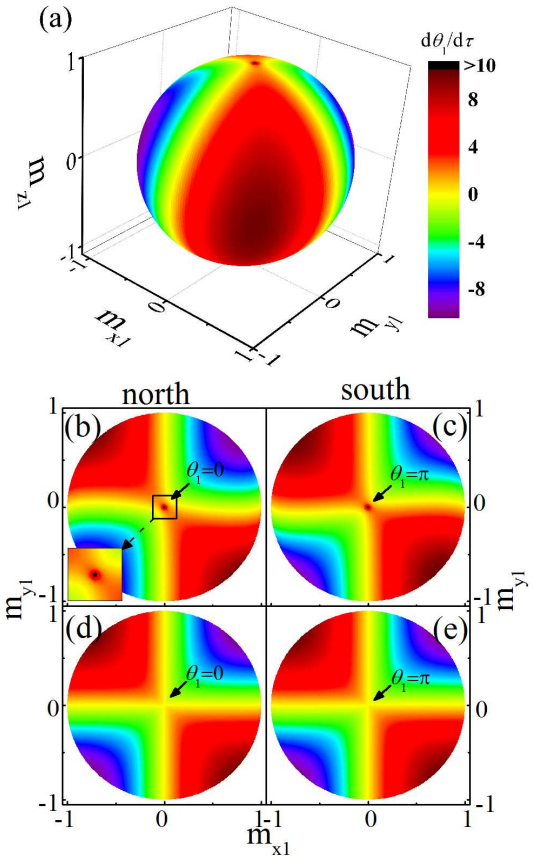

FIG. 2. The contour plot of $d\theta_1/d\tau$ on spherical surface of a symmetric junction, we fix $\mathbf{m_2}$ at the position $\theta_2 = 0.1\ \pi$ and $\phi_2 = 0$. (a) 3D view with α_1'=α_2'=0.1, (b) and (c) are the top and bottom view of (a), respectively. (d) and (e) are the top and bottom view for the case of α_1'=α_2'=0.

ically, we set the saturation magnetization to be $M_{s,1} = M_{s,2} = 1$ T, the dimensionless planar anisotropy to be $h_{p,1} = h_{p,2} = 20$, the uniaxial anisotropy field to be $H_{k,1} = 250$ Oe, the asymmetric field parameter to be $k = k_2/k_1$ for convenience, and the intrinsic magnetic damping coefficient to be $\alpha_{0,1} = \alpha_{0,2} = 0.01$, and the enhanced magnetic damping coefficient α_1' and α_2' to be ranged from 0.0025 to 0.12 according to the first-principles calculations.[23] We take a same thickness $d_1 = d_2 = 2$ nm for both the FM layers and ignore the effect of the out-of-plane STT which is about one-fifth of the in-plane STT. $\Lambda = 1$[61] is taken for the electric-bias-induced STT and $\Lambda = 3.55$[41] is chosen for TSTT. The ferromagnetic resonance frequency $1/\tau_1 \sim 1/216$ps is estimated for the left magnetization $\mathbf{m}_1$.

A. Free spin dynamics

The spin dynamics in $FM_1|I|FM_2$ junction is time dependent. When the FM_2 magnetization begins to process, FM_1 would be driven by the spin current pumped from FM_2. A stable procession would be developed when the external driving force compensates with the intrinsic damping.

It is useful to take a snapshot of the angular dependent velocity of the left magnetization by solving the coupled LLG equations, and the corresponding results for α'=0.1 and α'=0 are shown in Fig. 2. Here, we fix the magnetization of the right side to be 0.1 π deviated from the equilibrium state. The static solution can be obtained from Eq. 1, which satisfies $\dot{\theta}_1 = 0$ and $\dot{\phi}_1 = 0$ simultaneously. Fig. 2 (b) and (c) are the projective views of Fig. 2 (a) along the z and $-z$ axis, respectively. $\dot{\theta}_1 \to \infty$ is obtained for $\theta_1 = 0$, demonstrating that the magnetization could not stand at the north, while $\dot{\theta}_1 \to \infty$ for $\theta_1 = \pi$ indicates that the magnetization tends to align along the south pole. Two yellow strips separate the red (positive $\dot{\theta}_1$) and purple (negative $\dot{\theta}_1$) regions, where the incoming spin current resulted from the processing FM_2 magnetization would cancel out that resulted from the FM_1, resulting in a metastable state. The planar anisotropy in FM_1 layer destroys the rotational symmetry, resulting in a mirror symmetry. Moreover, the singularity always exist in the north and south poles, respectively, regardless of how weak is the spin pumping effect, demonstrating that the spin pumping destabilizes the P state and stabilizes the AP state. As the spin pumping effect diminishes to zero, the singularities are completely disappeared, as clearly shown in Fig. 2 (d) and (e).

Then, we pay our attention to the relaxation time which characterizes how fast a stable procession can be reached. To estimate the relaxation time, we introduce a normalized magnetoresistivity

$$r = \frac{1 - cos^2(\theta_{12}/2)}{1 + cos^2(\theta_{12}/2)} \tag{3}$$

where θ_{12} is the relative angle between $\mathbf{m}_1$ and $\mathbf{m}_2$, and the order parameter $s = (\theta_1 + \theta_2)/\pi$. It is noted that in the tunnel junction or spin valve, $r \to 1$ is with a high resistivity, while $r \to 0$ is with a low resistivity. $s \to 1$ and $s \to 0$ are obtained for the AP state and P state, respectively. Considering an initial state with $r \neq 0$ and $s \neq 0$, the critical relaxation time t_c is defined as the time needed for r decreases to 0/1 ($t_{c,r}$) or s increases to 0/1 ($t_{c,s}$).

Figure 3(a) and (b) show two typical relaxation processes to the P state and AP state, respectively. First, we study the relaxation to the P state. When both the magnetizations are processing under the identical effective fields, i.e., $k = 1$, $t_{c,r} \sim 0.2\ \mu$s and $t_{c,s} \sim 15\ \mu$s are estimated, demonstrating that the critical time for the the coherent procession is considerable shorter than that for reaching to the stable focus. Comparatively, $t_{c,r}$ is close to $t_{c,s}$ for the effective fields with significant different magnitudes , i.e., $k \gg 1$ or $k \ll 1$, as shown in the inset of Fig. 3 (a) and Table I. On the other hand, considerable differences between $t_{c,r}$ and $t_{c,s}$ are observed both for the identical effective fileds case and for the different effective fileds case. Furthermore, both $t_{c,r}$ and

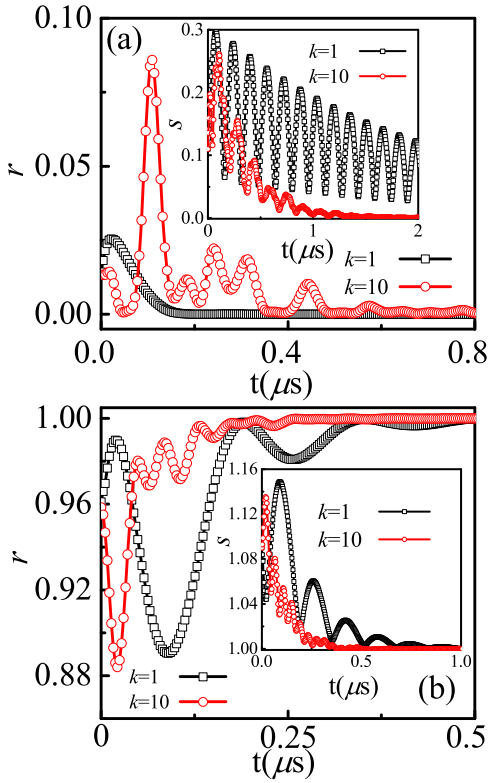

FIG. 3. The calculated normalized magnetoresistivity r and order parameter s as a function of time t for the relaxation to the (a) P and (b) AP state after disturbance. We set the initial parameters to be $\theta_1 = 0.01\ \pi$ and $\phi_1 = 0$ for both the P and AP states, and $\theta_2 = 0.1/0.9\ \pi$ and $\phi_2 = 0/0$ for the P/AP state.

TABLE I. The relaxation time $t_{c,r}/t_{c,s}$ in unit of μs in the magnetic structure with the initial position $\theta_1 = 0.01\pi/0.99\pi$, $\phi_1 = 0/0$, $\theta_2 = 0.1\pi/0.1\pi$, and $\phi_2 = 0.5\pi/0.5\pi$ for the relaxation to the P/AP state.

structure	$\alpha' = 0$		$\alpha' = 0.1$	
	$k = 1$	$k = 10$	$k = 1$	$k = 10$
P	8/15	6/12	0.2/15	1.2/2.5
AP	8/15	6/12	0.8/1.3	0.7/0.9

$t_{c,s}$ are comparatively smaller than those of the relaxation to the P state, respectively. When the spin pumping effect is completely diminished, $t_{c,r} \sim 8/6\ \mu$s and $t_{c,s} \sim 15/12\ \mu$s are estimated for $k = 1/10$, as given in Table I, which are one order longer respectively than those with the spin pumping effect. Thus, it is indicated that spin pumping for a asymmetric effective field accelerates the relaxation. Moreover, the waving curve is observed for a large asymmetric effective field due to the strong dynamical exchange coupling therein.

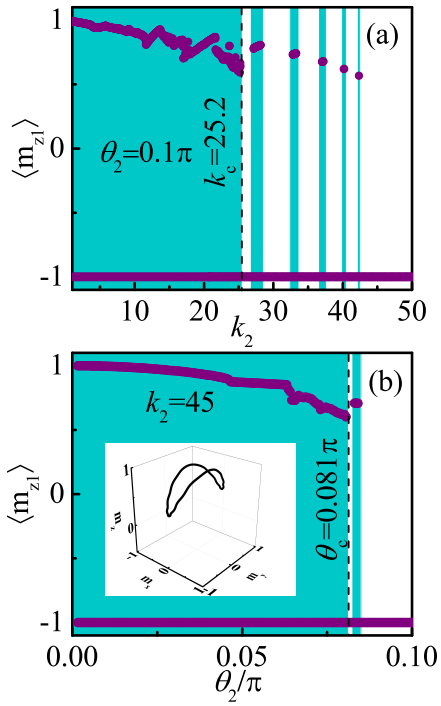

FIG. 4. (a) $< \mathbf{m}_{z1} >$ as a function of effective filed k_2 at precessing cone angle θ_2=0.1π, and (b) $< \mathbf{m}_{z1} >$ as a function of θ_2 with $k_2 = 45$. Therein, we take the enhanced magnetic damping coefficient $\alpha_1' = 0.1$.

B. Dynamical exchange coupling with a stable processing magnetization

Subsequently, we study the spin dynamics under the effect of the dynamical exchange coupling with a stable processing magnetization. The experimental realization could be in the $FM_1|I|FM_2$ junction with a ferromagnetic resonance frequency of FM_2 magnetization coinciding with the frequency of the external magnetic field, while that of the other magnetization FM_1 detunes from the frequency of the external magnetic filed. The precession cone angle can be tuned by the importing power from a ferromagnetic resonance (FMR) equipment such as a microwave radio frequency field.

Here, we assume that FM_2 precesses with the coherent frequency $\Omega_{K,2}$ and cone angle θ_2. When the dynamical exchange coupling gets involved, the normalized magnetoresistivity is time dependent. Considering a $FM_1|I|FM_2$ junction, the time average of the normalized magnetoresistivity is proportional to that of the z component of the magnetization m_1 ($< m_{z1} >$). Here, over 50 various $\mathbf{m}_1$ with a uniform probability distribution are used to get a reasonable estimation.

Figure 4 gives the dependence of $< m_{z1} >$ on the effective field and processing cone angle of the FM_2 magnetization. There is one solution in various k_2 regions (white area) and two solutions in the remaining k_2 regions (blue area). Thus, the state of $< m_{z1} >= -1.0$ is further

stabilized by the effective field and the processing cone angle of the right magnetization θ_2, consistent with the calculated angular dependent velocity of the left magnetization shown in Fig. 2. The state of $< m_{z1} >= 1.0$ only exists in the absence of the spin pumping effect (k_2=0 or θ_2=0), and the magnetization would be reversed to the $-z$ axis when the spin torque pumped by the precessing $\mathbf{m}_2$ compensates with the damping torque. Owing to the planar anisotropy, a in-plane precession (IPP) structure (the inset of Fig. 4 (b)) is observed in the blue regions in Fig. 4 for the initial quasi-P configurations. Thus, it is demonstrated that the spin pumping favors the P to AP switching rather than the AP to P switching.

Furthermore, several critical k_2 are observed as shown in Fig. 4 (a) which gives the calculated $< m_{z1} >$ for $\theta_2 = 0.1\ \pi$. The minimal critical k_2 is estimated to $k_c \sim 25.2$. In some extant, the presence of several critical k_2 is related to the cooperation of the amplitude and working frequency of the dynamic spin current pumped by the precessing FM_2 magnetization. As k_2 increases, the region between two neighboring critical k_2 becomes narrower, indicating that the effect of the frequency becomes less important when the spin current amplitude is strong enough. Then, the calculated $< m_{z1} >$ as a function of cone angle θ_2 for $k_2 = 45$ is shown in Fig. 4 (b). Similarly, more than one critical θ_2 are observed, and the minimal one is estimated to be $\theta_c \sim 0.81\pi$. Interestingly, it is estimated that the switching time from the P state to the AP state is as short as ~ 2 ns (although the corresponding results are not shown here), which is related to the high effective field under $H_{k,2} = 11.25$ kOe.

C. Spin dynamics with external spin torque

For the spin torque pumped by the processing magnetization favors the switch from the P state to the AP state rather than the reversed one, an external spin torque should be applied to overcome the damping torque and spin pumping torque in order to achieve the switch from the AP state to the P state. In this subsection, we study the effect of external spin torque on the spin dynamics in FM_1|I|FM_2 MTJs with a stable processing magnetization. It is noted that an electronic voltage or thermal bias across the insulator could drive a spin polarizing current and exert a spin torque.

Figure 5 gives the calculated $\mathbf{m}_1$ as a function of the precessing cone angle of $\mathbf{m}_2$ and the external spin torque for the P to AP switching (left column) and for the AP to P switching (right column) for various enhanced magnetic damping coefficient α_1' ranged from 0.005 to 0.04 at $k_2 = 50$. As α_1' increases, the θ_2 region with the AP state (blue area) becomes larger, indicating that the spin pumping favors the AP state rather than the P state. For small $\alpha_1' = 0.005$ [Fig. 5 (a) and (d)], an external spin torque around $-8.0(8.0)$ μJ/m^2 can switch $\mathbf{m}_1$ from the P (AP) state to the AP (P) state. A larger external spin torque is needed to reverse the magnetization of FM_1 as

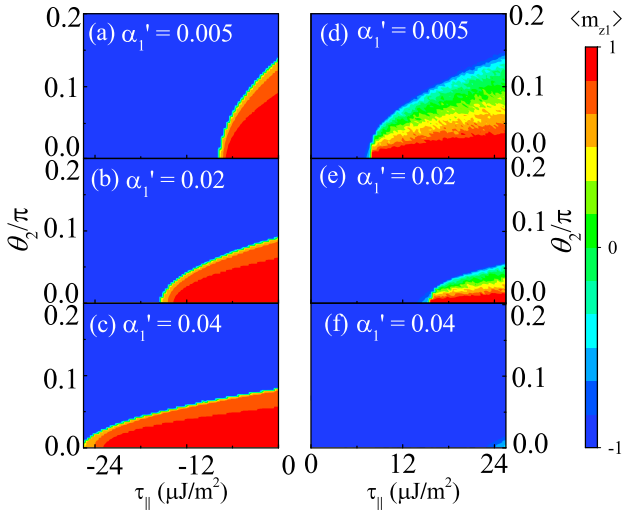

FIG. 5. The contour plot of $<m_{z1}>$ on the ($\tau_\parallel$, θ_2) parameter plane for fixed $k_2 = 50$ with various α_1', $\Lambda = 1$ is taken for $\tau_\parallel$. $\mathbf{m}_1$ was set initially around (a-c) north pole and (d-f) south pole. The blue/red areas means that the AP/P state is stable.

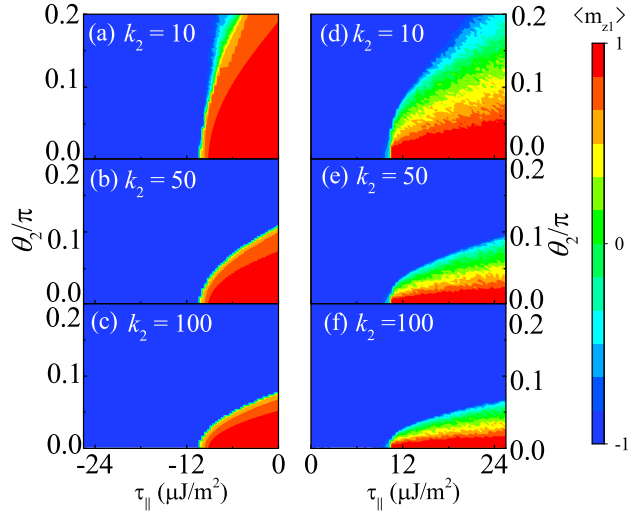

FIG. 6. The contour plot of $< m_{z1} >$ on the ($\tau_\parallel$, θ_2) parameter plane for fixed α_1'=0.01 with various k_2. Calculation details are the same as those in Fig. 5.

α_1' increases.

Figure 6 gives the calculated results for various k_2 ranged from 10 to 100 at $\alpha_1' = 0.01$. It is clearly shown that the P state can be gradually replaced by the AP state with the increase of k_2, indicating that modulating k_2 (for a fixed precessing cone angle θ_2) is an effective method to reduce the critical exterior spin torque in reversing the magnetization. However, k_2 shows less effect on the AP to P switching, comparing with that on the P to AP switching.

For a clean Fe|MgO|Fe MTJs with 3 layers barrier, a large skewed angular dependence on TSTT would favor

the AP to P switching.[41] For a small dynamical exchange coupling $\alpha_1' = \alpha_2' = 0.005$, a exterior spin torque around 2.5 $\mu J/m^2$ at a relative angle of 90° can switch the AP state to the P state in the absence of the spin pumping torque, and a large spin torque around 11.5 $\mu J/m^2$ is needed to switch the P state to the AP state. For the TSTT induced by the hot flowing electrons has an exponential correlation with the thickness of the barrier, junctions with MgO thickness less than 2 monolayers favor thermal magnetization switch considering the current experimental capacity, where the instantaneous temperature bias less than 10 K can be obtained by a laser heater. Moreover, TSTT induced by a hot magnon, which is proportional to the enhanced magnetic damping coefficient, can switch the magnetization with the temperature bias $\sim$ 10 K.[45] For a thicker MgO barrier junction, the bias-induced-STT is expected, while TSTT can not switch the magnetization alone. The spin pumping torque, whose magnitude is determined by the processing cone, effective field and enhanced magnetic damping coefficient as discussed in detail above, has a effect on the spin dynamics similar to that of the TSTT or bias-driven-STT, and can be used to prompt the magnetization switch in magnetic nano-structures.

IV. SUMMARY

In summary, we study the spin dynamics in Fe|MgO|Fe MTJs with the dynamical exchange coupling by LLG equations. Free spin dynamics studies show that the quasi-antiparallel structure is more stable than the quasi-parallel structure in the presence of spin pumping. The effects of the processing cone angle, the asymmetric effective field, and the external spin torque on the magnetic state switching are investigated in detail. It is demonstrated that the spin pumping torque can efficiently modulate the magnetization switch, similar to the TSTT and bias-driven-STT. Thus, it is strongly suggested that the spin pumping torque can be used as another parameter to modulate the spin dynamics in magnetic nano-structures. Hence, our work demonstrates the important role of the spin pumping on the magnetization switch, and provides a new insight for future experiments and the corresponding device design.

V. ACKNOWLEDGEMENT

We gratefully acknowledge financial support from National Natural Science Foundation of China under the grant No. 11274094 and 51332007, and the National Key Projects for Basic Research of China under the grant No. 2015CB921202. X.J. also acknowledge financial support from HPU with grant No. B2012-021 and T2016-2.

* jiaxingtao@hpu.edu.cn
† qinmh@scnu.edu.cn

[1] S. K. Kim, O. Tchernyshyov, and Y. Tserkovnyak, Phys. Rev. B **92**, 020402(R) (2015), URL https://journals.aps.org/prb/abstract/10.1103/PhysRevB.92.020402.
[2] T. Erlend G, A. Qaiumzadeh, and A. Brataas, Phys. Rev. Lett **112**, 147204 (2014), URL https://journals.aps.org/prl/abstract/10.1103/a.112.147204.
[3] S. Selzer, U. Atxitia, U. Ritzmann, D. Hinzke, and U. Nowak, Phys. Rev. Lett **117**, 107201 (2016), URL https://journals.aps.org/prl/abstract/10.1103/PhysRevLett.117.107201.
[4] S. K. Kim, D. Hill, and Y. Tserkovnyak, Phys. Rev. Lett **117**, 237201 (2016), URL https://journals.aps.org/prl/abstract/10.1103/PhysRevLett.117.237201.
[5] V. S. Gerasimchuk, Y. I. Gorobets, and S. Goujon-Durand, Phys. Rev. B **49**, 9608 (1994), URL https://journals.aps.org/prb/abstract/10.1103/PhysRevB.49.9608.
[6] M. Stamenova, R. Mohebbi, J. Seyed-Yazdi, I. Rungger, and S. Sanvito, Phys. Rev. B **95**, 060403(R) (2017), URL https://journals.aps.org/prb/abstract/10.1103/PhysRevB.95.060403.
[7] Y. Liu, Z. Yuan, R. J. H. Wesselink, A. A. Starikov, and P. J. Kelly, Phys. Rev. Lett. **113**, 207202 (2014), URL http://link.aps.org/doi/10.1103/PhysRevLett.113.207202.
[8] S. Mizukami, Y. Ando, and T. Miyazaki, Jpn. J. Appl. Phys. **40**, 580 (2001), URL http://stacks.iop.org/1347-4065/40/i=2R/a=580.
[9] S. Mizukami, Y. Ando, and T. Miyazaki, Journal of Magnetism and Magnetic Materials **226–230, Part 2**, 1640 (2001), ISSN 0304-8853, proceedings of the International Conference on Magnetism (ICM 2000), URL http://www.sciencedirect.com/science/article/pii/S0304885300010970.
[10] W. H. Butler, X.-G. Zhang, T. C. Schulthess, and J. M. MacLaren, Phys. Rev. B **63**, 054416 (2001), URL http://link.aps.org/doi/10.1103/PhysRevB.63.054416.
[11] J. Mathon and A. Umerski, Phys. Rev. B **63**, 220403 (2001), URL http://link.aps.org/doi/10.1103/PhysRevB.63.220403.
[12] Y. Ke, K. Xia, and H. Guo, Phys. Rev. Lett. **105**, 236801 (2010), URL http://link.aps.org/doi/10.1103/PhysRevLett.105.236801.
[13] M. Walter, J. Walowski, V. Zbarsky, M. Münzenberg, M. Schäfers, D. Ebke, G. Reiss, A. Thomas, P. Peretzki, J. S. Seibt, Michael andMoodera, et al., Nat. Mater. **10**, 742 (2011).
[14] N. Liebing, S. Serrano-Guisan, K. Rott, G. Reiss, J. Langer, B. Ocker, and H. W. Schumacher, Phys. Rev. Lett. **107**, 177201 (2011), URL http://link.aps.org/doi/10.1103/PhysRevLett.107.177201.

[15] M. Czerner, M. Bachmann, and C. Heiliger, Phys. Rev. B **83**, 132405 (2011), URL http://link.aps.org/doi/10.1103/PhysRevB.83.132405.

[16] W. Lin, M. Hehn, L. Chaput, B. Negulescu, S. Andrieu, F. Montaigne, and S. Mangin, Nat. Commun. **3**, 744 (2012).

[17] M. Czerner and C. Heiliger, J. Appl. Phys. **111**, 07C511 (2012).

[18] A. Boehnke, M. Milnikel, M. von der Ehe, C. Franz, V. Zbarsky, M. Czerner, K. Rott, A. Thomas, C. Heiliger, G. Reiss, et al., Sci. rep. **5**, 8945 (2015).

[19] Z. Zhang, Y. Gui, L. Fu, X. Fan, J. Cao, D. Xue, P. Freitas, D. Houssameddine, S. Hemour, K. Wu, et al., Phys. Rev. Lett. **109**, 037206 (2012).

[20] J. Teixeira, J. Costa, J. Ventura, M. Fernandez-Garcia, J. Azevedo, J. Araujo, J. Sousa, P. Wisniowski, S. Cardoso, and P. Freitas, Appl. Phys. Lett. **102**, 212413 (2013).

[21] P. Ogrodnik, G. E. W. Bauer, and K. Xia, Phys. Rev. B **88**, 024406 (2013), URL http://link.aps.org/doi/10.1103/PhysRevB.88.024406.

[22] J. Xiao, A. Zangwill, and M. D. Stiles, Phys. Rev. B **72**, 014446 (2005), URL https://journals.aps.org/prb/abstract/10.1103/PhysRevB.72.014446.

[23] X. Jia, H. Tang, Z. Yuan, K. Xia, and G. E. W. Bauer (2017), unpublished.

[24] A. A. Baker, A. I. Figueroa, D. Pingstone, V. K. Lazarov, G. Van Der Laan, and T. Hesjedal, Scientific reports **6**, 35582 (2016), URL https://www.nature.com/articles/srep35582.

[25] W. Chen, M. J. Rooks, N. Ruiz, J. Z. Sun, and A. D. Kent, Phys. Rev. B **74**, 144408 (2006), URL https://journals.aps.org/prb/abstract/10.1103/PhysRevB.74.144408.

[26] T. Taniguchi and H. Imamura, Phys. Rev. B **78**, 224421 (2008), URL https://journals.aps.org/prb/abstract/10.1103/PhysRevB.78.224421.

[27] S. Takahashi, Appl. Phys. Lett. **104**, 052407 (2014).

[28] H. Skarsv?g, G. E. Bauer, and A. Brataas, Phys. Rev. B **90**, 054401 (2014), URL https://journals.aps.org/prb/abstract/10.1103/PhysRevB.90.054401.

[29] J. C. Slonczewski, J. Magn. Magn. Mater. **159**, L1 (1996).

[30] L. Berger, Phys. Rev. B **54**, 9353 (1996), URL http://link.aps.org/doi/10.1103/PhysRevB.54.9353.

[31] M. D. Stiles and A. Zangwill, Phys. Rev. B **66**, 014407 (2002), URL http://link.aps.org/doi/10.1103/PhysRevB.66.014407.

[32] J. C. Sankey, Y. T. Cui, J. Z. Sun, J. C. Slonczewski, R. A. Buhrman, and D. C. Ralph, Nat. Phys. **4**, 67 (2007).

[33] A. M. Deac, A. Fukushima, H. Kubota, H. Maehara, Y. Suzuki, S. Yuasa, Y. Nagamine, K. Tsunekawa, D. D. Djayaprawira, and N. Watanabe, Nat. Phys. **4**, 803 (2008).

[34] S.-C. Oh, S.-Y. Park, A. Manchon, M. Chshiev, J.-H. Han, H.-W. Lee, J.-E. Lee, K.-T. Nam, Y. Jo, Y.-C. Kong, et al., Nat. Phys. **5**, 898 (2009).

[35] H. Kubota, A. Fukushima, K. Yakushiji, T. Nagahama, S. Yuasa, K. Ando, H. Maehara, Y. Nagamine, K. Tsunekawa, and D. D. Djayaprawira, Nat. Phys. **4**, 37 (2008).

[36] C. Heiliger and M. D. Stiles, Phys. Rev. Lett. **100**, 186805 (2008), URL http://link.aps.org/doi/10.1103/PhysRevLett.100.186805.

[37] Z. Li and S. Zhang, Phys. Rev. B **69**, 134416 (2004), URL http://link.aps.org/doi/10.1103/PhysRevB.69.134416.

[38] J. C. Slonczewski, Phys. Rev. B **82**, 054403 (2010), URL http://link.aps.org/doi/10.1103/PhysRevB.82.054403.

[39] J. Xiao, G. E. W. Bauer, K.-c. Uchida, E. Saitoh, and S. Maekawa, Phys. Rev. B **81**, 214418 (2010).

[40] T. Taniguchi and H. Imamura, Phys. Rev. B **83**, 054432 (2011).

[41] X. Jia, K. Xia, and G. E. W. Bauer, Phys. Rev. Lett. **107**, 176603 (2011), URL http://link.aps.org/doi/10.1103/PhysRevLett.107.176603.

[42] G. E. Bauer, E. Saitoh, and B. J. van Wees, Nat. Mater. **11**, 391 (2012).

[43] M. Weiler, M. Althammer, M. Schreier, J. Lotze, M. Pernpeintner, S. Meyer, H. Huebl, R. Gross, A. Kamra, J. Xiao, et al., Phys. Rev. Lett. **111**, 176601 (2013), URL http://link.aps.org/doi/10.1103/PhysRevLett.111.176601.

[44] A. Pushp, T. Phung, C. Rettner, B. P. Hughes, S.-H. Yang, and S. S. Parkin, Proceedings of the National Academy of Sciences **112**, 6585 (2015).

[45] H.-M. Tang, X.-T. Jia, and S.-Z. Wang, Front. Phys. **12**, 128501 (2017).

[46] J. C. Leutenantsmeyer, M. Walter, V. Zbarsky, M. Münzenberg, R. Gareev, K. Rott, A. Thomas, G. Reiss, P. Peretzki, H. Schuhmann, et al., in *Spin* (World Scientific, 2013), vol. 3, p. 1350002.

[47] X. Jia, S. Wang, and M. Qin, New J. Phys. **18**, 063012 (2016).

[48] X. Jia, S. Wang, and M. Qin, New J. Phys. **18**, 063028 (2016).

[49] X. Wang, G. E. Bauer, B. J. van Wees, A. Brataas, and Y. Tserkovnyak, Phys. Rev. Lett. **97**, 216602 (2006), URL https://journals.aps.org/prl/abstract/10.1103/PhysRevLett.97.216602.

[50] M. V. Costache, M. Sladkov, S. M. Watts, C. H. van Der Wal, and B. J. Van Wees, Phys. Rev. Lett. **97**, 216603 (2006), URL https://journals.aps.org/prl/abstract/10.1103/PhysRevLett.97.216603.

[51] K. Jeon, B. C. Min, A. Spiesser, H. Saito, S. Shin, S. Yuasa, and R. Jansen, Nat. Mater. **13**, 360 (2014).

[52] Y. Tserkovnyak, A. Brataas, and G. E. W. Bauer, Phys. Rev. B **66**, 224403 (2002).

[53] Y. Tserkovnyak, A. Brataas, and G. E. W. Bauer, Phys. Rev. Lett. **88**, 117601 (2002).

[54] B. Heinrich, Y. Tserkovnyak, G. Woltersdorf, A. Brataas, R. Urban, and G. E. Bauer, Phys. Rev. Lett. **90**, 187601 (2003).

[55] Y. Tserkovnyak, A. Brataas, and G. Bauer, J. Appl. Phys. **93**, 7534 (2003).

[56] H. Jiao and G. E. W. Bauer, Phys. Rev. Lett. **110**, 217602 (2013), URL http://link.aps.org/doi/10.1103/PhysRevLett.110.217602.

[57] J. Li, L. R. Shelford, P. Shafer, A. Tan, J. X. Deng, P. S. Keatley, C. Hwang, E. Arenholz, G. van der Laan, R. J. Hicken, et al., Phys. Rev. Lett. **117**, 076602 (2016), URL http://link.aps.org/doi/10.1103/PhysRevLett.117.076602.

[58] J. Z. Sun, Phys. Rev. B **62**, 570 (2000), URL https://journals.aps.org/prb/abstract/10.1103/PhysRevB.62.570.

[59] T. Taniguchi and H. Imamura, Phys. Rev. B **76**, 092402 (2007), URL https://journals.aps.org/prb/abstract/10.1103/PhysRevB.76.092402.

[60] J. Slonczewski, J. Magn. Magn. Mater. **247**, 324 (2002), ISSN 0304-8853, URL http://www.sciencedirect.com/

science/article/pii/S0304885302002913.

[61] X. Jia, K. Xia, Y. Ke, and H. Guo, Phys. Rev. B **84**, 014401 (2011), URL http://link.aps.org/doi/10.1103/PhysRevB.84.014401.